AN INTEGRATED CELLULAR AND SUB-CELLULAR MODEL OF CANCER CHEMOTHERAPY AND THERAPIES THAT TARGET CELL SURVIVAL

Alexis B. Cook

Department of Applied Mathematics
Brown University
182 George Street
Providence, RI 02906, USA

Daniel R. Ziazadeh and Jianfeng Lu

Department of Internal Medicine
University of Michigan
Ann Arbor, MI 48109, USA

Trachette L. Jackson

Department of Mathematics
University of Michigan
530 Church Street
Ann Arbor, MI 48109-1043, USA

Abstract. Apoptosis resistance is a hallmark of human cancer, and tumor cells often become resistant due to defects in the programmed cell death machinery. Targeting key apoptosis regulators to overcome apoptotic resistance and promote rapid death of tumor cells is an exciting new strategy for cancer treatment, either alone or in combination with traditionally used anti-cancer drugs that target cell division. Here we present a multiscale modeling framework for investigating the synergism between traditional chemotherapy and targeted therapies aimed at critical regulators of apoptosis.

1. **Introduction.** Since their approval for the treatment of cancer in the 1970s, platinum-based chemotherapeutic agents have been an essential part of the standard of care for lung, ovarian, colorectal, testicular, bladder and head and neck cancers [3]. Cisplatin is the most commonly used platinum chemotherapeutic agent, but it's efficacy is often compromised because of the substantial risk for severe toxicities[8, 21]. Despite increasing efforts in early diagnosis, aggressive surgical treatment and application of additional non-operative modalities that minimize side effects, the prognosis for many cancers is still dismal. For head and neck (HN) tumors, the sixth most common malignancy in the world [22], state- of-the-art treatment with anti-mitotic, platinum-based drugs, including cisplatin, still results in a 5-year disease-specific survival of approximately 60% [27]. Conventional therapies

for head and neck cancer patients have achieved maximal benefit. Further improvements in survival rates and quality of life will only result from the development of new strategies for treatment.

In order to improve outcomes for HN cancers, a substantial amount of research is now focusing on the molecular biology of the tumors in an attempt to selectively target pathways involved in carcinogenesis. Increased understanding of molecular mechanisms in the pathogenesis of HN cancer is leading to targeted manipulation of these pathways, and rational approaches to cancer therapy at the molecular level are now being developed. Some of the new approaches depend on tumor biology and aim specifically to inhibit tumor growth and metastasis by targeting the tumor microenvironment or vasculature (leaving normal cells unaffected), but others focus on specific protein or signal transduction pathways associated with tumor cell proliferation and survival [18].

Mounting evidence has demonstrated that the primarily intracellular, pro-survival proteins Bcl-2 and Bcl-xL, which are upregulated in a variety of tumor types, including HN, constitute unique and important therapeutic targets for cancer. Bcl-2 and Bcl-xL play a role in the survival of both tumor and vascular endothelial cells and have been implicated in chemotherapeutic resistance to cisplatin. To date, the only dual Bcl-2/Bcl-xL inhibitors that have advanced into clinical development are ABT-263 [30, 38] and ABT-199 [26]. However, [2] has recently designed a new class of potent and specific, small-molecule dual inhibitors of Bcl-2 and Bcl-xL. Preliminary evidence suggests that BM-1197 is their most promising lead. It has been shown to be highly effective on both head and neck and lung cancer cells [2]. In order to exploit the therapeutic potential of BM-1197, and to predict optimal doses and dose scheduling, it is essential to combine biological experimentation, mathematical modeling, and numerical simulation to understand the molecular basis of their synergistic action.

Here we develop a simple, yet useful multilevel modeling framework to understand the mechanisms underlying the anti-tumor effect of therapeutic inhibition of Bcl-2 and Bcl-xL alone and in combination with cisplatin. Even though the framework presented here represents an *in vitro* setting, it is general enough that it can easily be extended to include highly specific and broad range inhibitors of the Bcl family of proteins in vivo following [14]. As more intracellular data becomes available, and the cellular mechanism of action of chemotherapeutic drugs is better understood, the model can be modified to more fully capture the range of intracellular drug dynamics that mediate increased cell death and also play a role in drug resistance.

2. **Mathematical model development.** Achieving a unified understanding of the intracellular, cellular, and tissue level response of tumors to combination treatments involving traditional chemotherapy and molecular targeted approaches is a relatively unexplored territory in computational cancer research. Notably, this is precisely the level of detail that is necessary to accurately predict the therapeutic potential of novel molecular targets that can affect cells in multiple ways. Our goal is to develop a basic, adaptable modeling framework that describes treatment dynamics starting from sub-cellular processes, while simultaneously modeling cell population dynamics using a macroscopic level of description. We will build this *in vitro* model in several steps, first focusing on developing an intracellular model of cisplatin uptake. We then modify this model to describe tumor response to intracellular cisplatin that is bound to DNA. Next, we build a model for treatment with

BM-1197, a small molecule inhibitor of Bcl-2, and finally we integrate these models to investigate combination therapy.

Each model is calibrated with experimental data, either collected for this study or taken from the literature, that measures cell survival as a result of administration of either BM-1197, cisplatin, or combination treatment with both drugs. Figure 1 shows the results of original experiments performed in relation to this study. Here, UMSCC-74B head and neck squamous cancer cells (HNSCCs) were treated with varying concentrations of Cisplatin, BM-1197, or both. After four days, the cells were washed and counted; the percentage of cells that survived was then recorded. Combination treatment was found most effective, followed by treatment with BM-1197, with cisplatin treatment least effective.
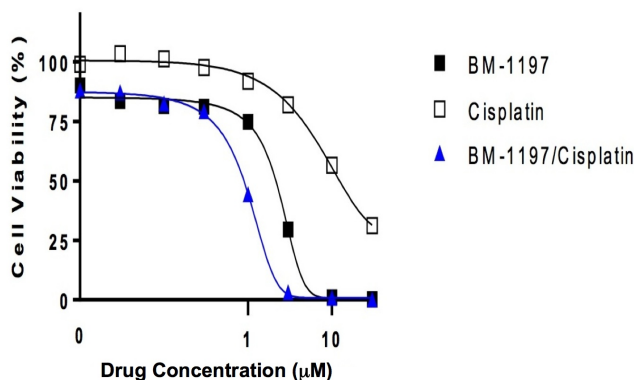

FIGURE 1. Cytotoxicity of Cisplatin, BM-1197, and Combination Treatment. UMSCC-74B is a University of Michigan generated head and neck squamous cell cancer cell line. Cell viability is plotted as a function of drug concentration: BM-1197 alone (black squares), cisplatin alone (white squares), and combination therapy corresponding to equal doses of cisplatin and BM-1197 (blue triangles).

2.1. **Intracellular cisplatin dynamics.** Cisplatin is a platinum-based chemotherapy agent that exerts its cytotoxic effect through binding to nuclear DNA. When cisplatin is administered to cells in vitro, it is believed to enter the cell through a combination of active and passive transport [31]. Once inside the cell, cisplatin binds to a variety of cellular targets. In particular, cisplatin can form adducts with DNA, inducing a cytotoxic distortion of the double helix that leads to programmed cell death. Reports of the proportion of intracellular bound cisplatin that is bound to DNA vary between 5-25%. This leaves approximately 75-95% of intracellular cisplatin free to associate with non-DNA targets [6, 16, 35].

As a first step to building a modeling framework for combination therapy with cisplatin and BM-1197, we first construct a model (equations 1a and 1b) that operates at the intracellular level and describes the kinetics of cisplatin uptake. We are interested in the time evolution of the quantity of intracellular cisplatin-DNA adducts, as it has been shown that cisplatin cytotoxicity is proportional to adduct concentration [36]. Although cells have evolved multiple mechanisms to repair cisplatin-damaged DNA and evade death, sufficiently high cisplatin doses, where the rate of DNA

platination exceeds the rate of DNA repair, can lead to an accumulation of damage, which can lead to cellular death.

The biological processes associated with cisplatin uptake and our simplified mathematical model are depicted in Figure 2.
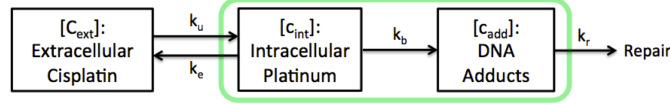

FIGURE 2. Cisplatin Intracellular Model.

Our *in vitro* model of intracellular cisplatin dynamics is adapted from [7] and Tables 1 and 2 define the variables and the parameters associated with the model. The initial parameter values were obtained by a best fit to the intracellular experimental data of [37].

Table 1: Definition of Variables for the Intracellular Cisplatin Model

Variable	Description	Units
C_{ext}	Extracellular Pt concentration	μg/ml [*]
c_{int}	Average intracellular non-DNA bound Pt conc. [†]	μg/ml [+]
c_{add}	Average concentration of Pt bound to DNA[†]	μg/ml[+]

[*] μg/ml, in terms of cell culture volume; [+] μg/ml, in terms of intracellular volume; [†] per cell

Table 2: Definition of Parameters for the Intracellular Cisplatin Model

Parameter	Description	Value	Source
k_u	Cisplatin uptake rate	0.1720 hr^{-1}	Best Fit[*]
k_e	Cisplatin efflux rate	0.4569 hr^{-1}	Best Fit[*]
k_b	DNA binding rate	2.042 hr^{-1}	Best Fit[*]
k_r	DNA repair rate	0.2232 hr^{-1}	Best Fit[*]

[*] The parameters are determined by a least squares fit to data in [37].

We assume that extracellular cisplatin C_{ext} is constant over the course of treatment, thus ignoring any binding to constituents of the culture medium. Cisplatin enters cells at the cellular uptake rate, k_u, and is removed from the cell at rate, k_e. Once inside the cell, intracellular cisplatin c_{int} associates with DNA to form adducts at the binding rate, k_b; and DNA adducts c_{add} are repaired at rate, k_r. Although cisplatin forms different types of DNA adducts including monoadducts, intrastrand adducts, and interstrand crosslinks (ICLs) [17], all cisplatin-DNA adducts are treated equally. The model equations are given below and the least squares, best fit to the intracellular cisplatin uptake data of [37] is shown in Figure 3.

$$\frac{dc_{int}}{dt} = k_u C_{ext} - k_e c_{int} \qquad (1a)$$

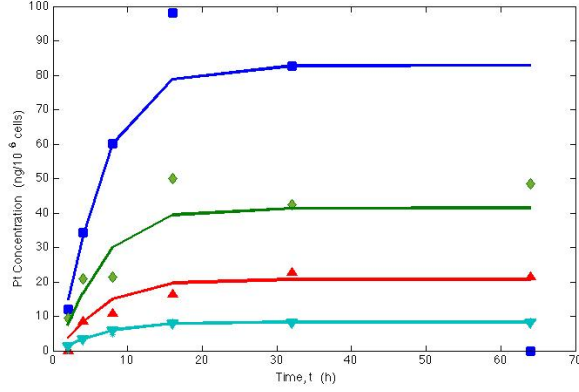$$\frac{dc_{add}}{dt} = k_b c_{int} - k_r c_{add} \qquad (1b)$$

FIGURE 3. Best fit of (1a, 1b) to experimental data in [37]. Blue corresponds to a 10 μg/ml external dose of cisplatin, green = 5 μg/ml, red = 2.5 μg/ml, and cyan = 1μg/ml. Note: The y-axis is the total Pt concentration inside the cell ($c_{int} + c_{add}$). The data was given in units of $\frac{ngPt}{10^6\ cells}$. In order to covert between these units and the units of our model we use cell volume of $2.17 \times 10^{-9} ml$ to obtain $\frac{ngPt}{10^6\ cells} = \frac{1}{2.17} \frac{\mu g\ Pt}{ml}$.

2.2. **Multiscale model of cisplatin treatment.** In the previous section, we see how a very simple model can capture the intracellular accumulation of cisplatin in cancer cells. We now move from the intracellular level to the cellular level by adding an equation describing the tumor's response to *intracellular* cisplatin-DNA adducts. The only new variable is $N \equiv$ total number of tumor cells, and its rate of change is given by:

$$\frac{dN}{dt} = \lambda N - \frac{\eta_0 c_{add}}{\eta_1 + c_{add}} N \qquad (2)$$

The parameter λ is rate of growth of cells in drug-free conditions, which takes into account natural cell death. We are ultimately interested in combination therapy applied to UMSCC-74B cells, which form aggressive tumors in nude mice. We therefore take the value of λ from estimates of the UMSCC-74B *in vitro* tumor doubling time, which was roughly 24 h (1 day). Cisplatin can induce cell death by both apoptosis and necrosis; however we only model the apoptotic mechanism here. This choice may be viewed as a simplifying assumption made in order to be consistent with the existing modeling literature [11, 12, 13] and to avoid the addition of several new parameters for which we have no data.

We do not have intracellular data for this cell line, so we must refit the full model (1a, 1b, 2) to data describing UMSCC-74B response to therapy. We are now in a data-limited situation (six parameters and only eight data points), and to compensate for this we retain two of the previous parameters (the cellular influx and efflux rates) from the Troger data in Table 2. Our rationale for making this choice is that there are significant differences from one cell line to another in DNA binding rates ($k_b \in (0.2024, 11.37)$ per hour as estimated in [7, 35]) and in the DNA repair rates ($k_r \in (0.0052, 1.441)$ per hour as estimated in [7, 35]). Therefore, we chose to re-estimate these two parameters in order to fit the data for the UMSCC-74B cells.

A third reason for retaining parameters from the previous fit is that the intracellular cisplatin model (Equation 1a and 1b) is time-dependent, yet the cytotoxicity data it is being fit to is time independent, as it is a dose-response curve for a single exposure time. This implies that the time scale for tumor growth should not enter into a fit to the data in Figure 1, which illustrates survival relative to untreated control cells. Therefore, in the absence of any further information about timescales (e.g. information obtained from the intracellular model), it would be impossible to determine all the parameter values for cisplatin treatment from data in Figure 1, as the time units would be arbitrary.

The new model parameters are presented in Table 3 and the best fit is shown in Figure 4.

Table 3: Parameter Values for the Cisplatin Treatment Model

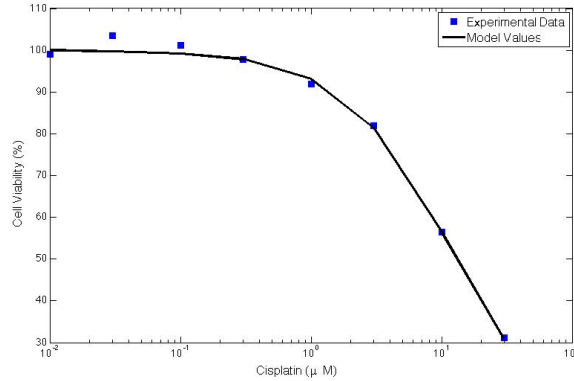| Parameter	Value	Source
k_u	0.1720×24 day^{-1}	Table 2
k_e	0.4569×24 day^{-1}	Table 2
k_b	11.24day^{-1}	Best Fit
k_r	3.903 day^{-1}	Best Fit
λ	0.6931 day^{-1}	UMSCC-74B Data
η_0	0.6368 day^{-1}	Best fit
η_1	33.80 μg/ml	Best fit

FIGURE 4. Best fit of the multi-scale mathematical model for cisplatin treatment in (1a, 1b, 2) to cell viability data for cisplatin in Figure 1. Here, the x-axis is the extracellular dose of Cisplatin.

The differences in the intracellular parameters can be attributed to the differences in DNA binding and repair that exist from cell line to cell line. We also note that there are could possibly be other parameter choices that could give good fits (in the least-squared sense). However, we searched parameter space for a defined, realistic range of parameters, and the reported local minimum was found.

2.3. **BM-1197 model.** Targeting key apoptosis regulators to overcome resistance and promote apoptosis of tumor cells is an exciting new strategy for cancer treatment [25, 28]. The Bcl-2 family of primarily intracellular proteins, which includes

anti-apoptotic (Bcl-2, Bcl-xL, Mcl-1) and pro-apoptotic (Bid, Bim, Bad, Bak, Bax) molecules, function as critical regulators of apoptosis in both cancer and normal cells [1, 5, 29]. While normal cells have low expression levels of the anti-apoptotic Bcl-2 and Bcl-xL proteins, these proteins are highly overexpressed in many tumors [1, 5]. This overexpression has been linked to poor prognosis in several types of cancer, and to clinical resistance to current cancer treatments [1, 5, 29]. The pro-survival proteins Bcl-2 and Bcl-xL are attractive targets for the development of anticancer therapies. For example, BM-1197 is a potent and specific small molecule inhibitor of Bcl-2/Bcl-xL that binds to both proteins with K_i values < 1 nM [2]. It effectively induces apoptosis in cancer cells and demonstrates strong apoptosis induction in tumor tissues *in vivo*. In fact, treatment with BM-1197 achieves complete and persistent tumor regression in animal models of human cancer, and evidence suggests that it is more efficacious than ABT-263, one of the only drugs of this type that has advanced to clinical trials [2].

Our model of BM-1197 therapy is based on the models of BL193 and ABT-737 presented in [11, 12, 13], where the Bcl family of proteins are assumed to be solely intracellular in order to keep the model relatively simple and the number of parameters at a minimum given limited experimental data. Tables 4 and 5 define the variables and the parameters associated with the model.

Table 4: Definition of Variables for the BM-1197 Model

Variable	Description	Units
N	Total number of tumor cells	#
B	Free Bcl-xL concentration	μg/ml
b	Free Bcl-xL per cell $\left(\frac{B}{N}\right)$	μg/ml
X	Unbound BM-1197 concentration	μg/ml
P	Bcl-xL-BM-1197 complex concentration	μg/ml

These are average concentrations in the cell culture well, i.e. μg/ml, in terms of cell culture volume.

The model equations are as follows:

a) No Therapy (Control)

$$\frac{dN}{dt} = \lambda N \tag{3}$$

b) BM-1197 Therapy

$$\frac{dN}{dt} = \lambda_n N - \delta(b)N \tag{4a}$$

$$\frac{dB}{dt} = \gamma(b)N - \lambda_b B + \lambda_n N b_s - k_1 BX + k_{-1}P - \delta(b)B \tag{4b}$$

$$\frac{dX}{dt} = -\lambda_x X - k_1 BX + k_{-1}P \tag{4c}$$

$$\frac{dP}{dt} = k_1 BX - k_{-1}P - \delta(b)P \tag{4d}$$

Before therapy is applied, tumors grow at an exponential rate (λ) that includes proliferation and natural cell death in drug-free medium as shown in (3). In this case, all cells instantaneously equilibrate to the constitutive level of Bcl-xL, $b =$

b_s, and no time-dependent equation for $B(t)$ or $b(t) = \frac{B}{N}$ is needed. BM-1197 therapy will affect the rate of cellular apoptosis. Therefore, when therapy is applied (see (4a)), tumor cells proliferate at their intrinsic division rate λ_n, which does not include natural cell death, and they die at rate δ, which varies with Bcl-xL concentration, b. Note that this implies that $\lambda = \lambda_n - \delta(b_s)$.

When treatment is applied, Bcl-xL levels dynamically vary due to BM-1197 binding. In the (4b) we see that Bcl-xL is produced by all tumor cells at rate γ that depends on the current intracellular concentration of Bcl-xL, b. It undergoes natural decay at a rate λ_b. Newly created cells (via proliferation) instantaneously establish a constitutive level, b_s, of free Bcl-xL. This represents an addition to the total Bcl-xL concentration B at rate $\lambda_n N b_s$, while cell death results in the loss of Bcl- xL at rate $\delta(b)$. Finally, free Bcl-xL may interact with the anticancer agent BM-1197 (X), a small molecule inhibitor of Bcl-xL. This interaction results in the formation of complexes (P), where k_1 is the forward rate of the reaction $B + X \rightleftharpoons P$, and k_{-1} is the backward rate.

BM-1197 undergoes natural decay at rate λ_x. Following [11, 12, 13], we make the assumption that since the cell membrane is highly permeable to small molecule inhibitors, BM-1197 is free to move in and out of cells, and when inside cells, it rapidly forms complexes (P) with Bcl-xL. The Bcl-2 family exert either a pro- or anti-apoptotic effect, they do not regulate necrosis, this means intracellular contents are not released into the extracellular space when death occurs. For this reason, we do not consider Bcl-xL or drug complexes to be recoverable in the extracellular pool upon cell death.

Table 5: Definition of Parameters for the BM-1197 Model

Parameter	Name	Value	Source
λ_n	Cell proliferation rate	0.6933 day^{-1}	[7]
b_s	Constitutive Bcl-xL level	$0.15 \times 10^{-3} \mu$M	[7]
λ_x	BM-1197 decay rate	0.4632 day^{-1}	Best Fit
k_1	BM-1197 association rate	86.4 μM/day	Best Fit
k_{-1}	BM-1197 dissociation rate	86.4 day^{-1}	Best Fit
ϵ_1	Cell death sensitivity	$\frac{b_s}{100} = 1.5 \times 10^{-6}$	

2.3.1. *Functional forms.* Appropriate functional forms for $\gamma(b)$ and $\delta(b)$ will critically depend on the cell line and small molecule inhibitor under consideration. Below we pay particular attention to known biology in order to derive functional forms that fit well with data on UMSCC-74B cells and BM-1197. In determining a form for $\gamma(b)$, the Bcl-xL production rate, we first note that in the drug-free (control) case we can rewrite the equation for B (free Bcl-xL concentration) in terms of b (free intracellular Bcl-xL as follows):

$$\frac{db}{dt} = \gamma(b) - \lambda_b b + \lambda_n (b_s - b.) \qquad (5)$$

In the absence of experimental data, a simple Hill function was chosen for $\gamma(b)$ in [12]. Their choice implies that the production rate of Bcl-xL is maximized if $b = 0$, and slows down as $b \to b_s$. Based on experimental evidence that treating cancer cells with cisplatin or with drugs that target the Bcl family of proteins can alter their long term intracellular anti-apoptotic protein levels [9, 19, 15, 23], we make

different assumptions here. We know that cancer cells should be able to settle to a steady state associated high levels of Bcl-xL, which corresponds to overexpression and increased survival. We are calling this steady state the constitutive level for tumor cells, b_s. There should also be a steady state that corresponds to the smaller, closer to normal levels Bcl-xL associated with levels attained before intrinsic and/or extrinsic perturbations resulted in overexpression. We will call this level of Bcl-xL, b_a. In order to achieve this, we would like for equation (5) to admit at least two stable steady states. Therefore, we will write:

$$\frac{db}{dt} = K(b_s - b)(b - b_1)(b - b_2). \qquad (6)$$

for some K, b_1, and $b_2 > 0$. Note, this assumes a very specific form for $\gamma(b)$. Without loss of generality, let $b_1 < b_2 < b_s$. Then b_1 and b_s represent stable steady states for Bcl-xL. Considering the implications of this choice of functional form, we note:

- If $b(t) \in (b_1, b_2)$, the cell will push Bcl-xL levels towards the level, b_1. To see this, consider $b(t) \approx b_2, b(t) < b_2$. Then initially, $b(t)$ decreases very slowly; as time progresses, the rate of decrease of $b(t)$ increases until it reaches a maximum. Eventually $b(t)$ begins to approach b_1 and the rate of change of $b(t)$ goes to zero.

- If $b(t) \in (b_2, b_s)$, the cell will push Bcl-xL levels towards the over expression state b_s. To see this, consider $b(t) \approx b_2, b(t) > b_2$. Then initially, $b(t)$ increases very slowly; as time progresses, the rate of increase of $b(t)$ increases until it reaches a maximum. Eventually $b(t)$ begins to approach b_s and the rate of change of $b(t)$ goes to zero.

In order for equations (5) and (6) to be consistent, we can write:

$$\frac{db}{dt} = (b_s - b) \left[K(b - b_a)(b - b_c) - \lambda_n \right] \qquad (7)$$

Using this functional form, the parameters $K, b_a, b_c > 0$ will be determined by a best fit to data.

The apoptotic cascade is an extremely complex series of events that is mediated by a wide variety of intracellular proteins. We therefore take a combined phenomenological and empirical approach for determining a functional form for the cell death rate, $\delta(b)$. First we examine the data and note that there is a very rapid drop in cell viability for small BM-1197 concentrations, followed by a plateau, and a second rapid decline in viability. We therefore represent $\delta(b)$ as the sum of two hyperbolic tangent functions in order to capture the two very distinct periods of rapid increase in cell death, which we hypothesize to reflect the sensitivity of the cell to Bcl-xL concentrations near the two stable steady states, b_s and b_a. Note that a variety of simpler choices for $\delta(b)$ were investigated; however, we found that these functional forms could not capture the large drop in cell viability for small drug concentrations that is characteristic of our data (see Figure 1) and the data presented in [2].

$$\delta(b) = h_1 \left[1 - \tanh\left(\frac{b - b_s}{\epsilon_1} \right) \right] + h_3 \left[1 - \tanh\left(\frac{b - b_a}{\epsilon_2} \right) \right] \qquad (8)$$

2.3.2. *Parameter estimation procedure.* Most parameters were taken from the literature; however, values for K, b_a, b_c and $\{h_i\}$ must be determined from available data. As mentioned above, the data suggests that there is a very rapid drop in

cell viability for small BM-1197 concentrations. Therefore, we first fit to the data points corresponding to the smallest concentrations of BM-1197 (.01-1 μM) to the first hyperbolic tangent function in (8). From this we find: $h_1 = 0.05961, b_c = 1.499 \times 10^{-4}, K = 1.006, b_a = 4.391 \times 10^{-6}$.

The data shows that the minimum value of b reached over the studied range of treatment options is roughly 0.7×10^{-4}. Therefore we can now modify $\delta(b)$ to the form presented in (8) by adding a function that is approximately equal to zero for $b \in [.7 \times 10^{-4}, b_s]$ without affecting the fit to data points corresponding to the smallest concentrations of BM-1197. This added function will ensure that the model achieves a good fit to the remaining three points. Refitting the model using (8) to the full set of cell survival data for treatment with BM-1197 gives $h_3 = 3.776, \epsilon_2 = 3.075 \times 10^{-5}$. Figure 5 shows the best fit to the data.
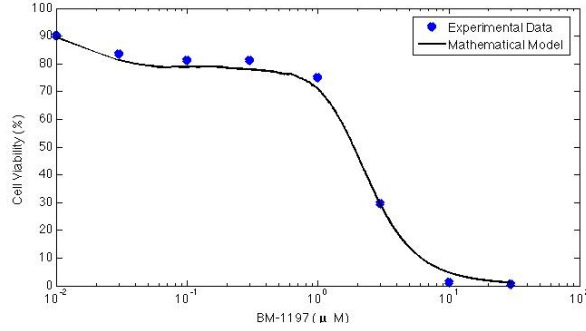

FIGURE 5. Best fit of the multi-scale mathematical model for BM-1197 treatment in (4) together with (7) and (8) to cell viability data for BM-1197 in Figure 1.

2.4. **Combination therapy.** We now integrate the model for chemotherapy (cisplatin) with the model for targeted therapy (BM-1197) to study combination treatment. The model equations are:

$$\frac{dN}{dt} = \lambda_n N - \delta(b)N - \eta(c_{add}, b)N \tag{9a}$$

$$\frac{dB}{dt} = \gamma(b)N - \lambda_b B + \lambda_n N b_s - k_1 BX + k_{-1}P - \delta(b)B \tag{9b}$$

$$\frac{dX}{dt} = \lambda_x X - k_1 BX + k_{-1}P \tag{9c}$$

$$\frac{dP}{dt} = k_1 BX - k_{-1}P - \delta(b)P \tag{9d}$$

$$\frac{dc_{int}}{dt} = k_u C_{ext} - k_e c_{int} \tag{9e}$$

$$\frac{dc_{add}}{dt} = k_b c_{int} - k_r c_{add} \tag{9f}$$

The full model differs from the previously published models in that we are assuming cells with cisplatin-induced DNA damage experience death at a rate $\eta(c_{add}, b)$ that depends on both intracellular cisplatin adducts and on the dynamically varying

intracellular Bcl-xL levels, b. We define this death rate as follows:

$$\eta_c\left(c_{add}, b\right) = \frac{\eta_0 c_{add}}{\eta_1 + c_{add}} \phi(b) \tag{10a}$$

$$\phi(b) = a_1 + 1 - a_1 \tanh\left(\frac{b + a_2}{\epsilon}\right) \tag{10b}$$

This choice of functional form is based on the assumption that there is a threshold above which Bcl-xL levels do not affect rate of cisplatin induced death. A best fit to the combination therapy data is given in Figure 6.
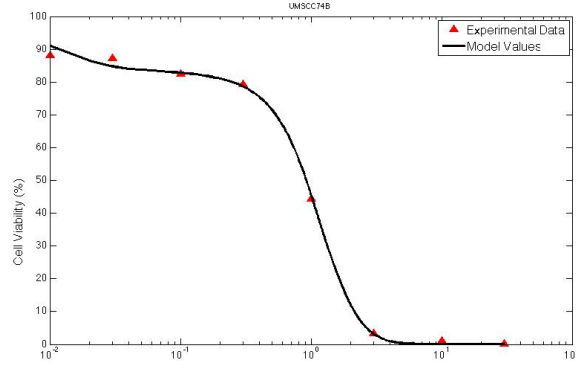

FIGURE 6. Best fit of the multi-scale mathematical model for combination treatment with both cisplatin and BM-1197 given in (9) and (10) to cell viability data for combination therapy in Figure 1.

3. **Optimizing treatment.** In the previous sections, we constructed and calibrated a model for BM-1197 therapy alone and in combination with cisplatin. Now we simulate different dose-scheduling regimens in order to investigate synergism between the two therapies. As can be seen in Figure 7, UMSCC-74B cells are treated with a range of concentrations of cisplatin for a period of 24 hours and then the cells are pretreated, co-treated, or post-treated with 0.4 or 0.8 μM BM-1197. Following the convention in [12], rectangular boxes indicate the addition of new drug and removal of any drug previously added. In Figure 7, IC50 corresponds to the computed cisplatin concentration required to produce 50% cell viability when combined with the specified dose of BM-1197. We quantified the therapeutic efficacy of various dosing strategies by taking the ratio of the predicted IC50 for each drug schedule (column 4 in Figure 7) with the control case (row 3 in Figure 7), where cells are co-treated with both Cipslatin and one, two, or three doses of BM-1197 for 24h. We call this metric the dose scheduling index (S. I.) and this ratio is the number reported in the last column of Figure 7. Smaller values of the S.I. denote optimal, synergistic treatment strategies, and S.I. values greater than 1 indicate some level of antagonism between the two drugs. Treatment of UMSCC-74B cells with cisplatin, followed by post-treatment with BM-1197, is preferred over pretreatment and co-treatment with BM-1197 as an optimal dosing strategy. The model predicts that cisplatin sensitizes cancer cells for treatment with BM-1197.

Day 1	Day 2 (Cisplatin)	Day 3	Day 4	Calculated IC50	S. I.
		BM-1197		34	0.36
	BM-1197	BM-1197		25	0.44
	BM-1197			94, 56, 14	1
BM-1197				85	0.90
BM-1197	BM-1197			70	1.2
BM-1197	BM-1197	BM-1197		17	1.2
		BM-1197	BM-1197	31	0.55
		2 x BM-1197		15	0.26
2 x BM-1197				47	0.84

FIGURE 7. Results from simulations to determine optimal treatment strategies and the potential for drug synergy. Here, cells are treated with cisplatin for a period of 24 hours (day 2) and then either pre-treated, co-treated, or post-treated with 0.4 or 0.8 μM BM-1197. Rectangular boxes indicate the addition of new drug and removal of any drug previously added. IC50 refers to the computed cisplatin concentration required to produce 50% cell viability when combined with the specified dose of BM-1197. The scheduling index, S.I., is the ratio of the predicted IC50 for each drug schedule (column 4) with the control case (row 3, blue box).

4. **Discussion.** The most important feature of this modeling framework is its flexibility to be extended in several directions. For example, although we did not have detailed intracellular data for UMSCC-74B cells, had that data been available we could have modified the intracellular cisplatin model to capture more molecular-level details of cisplatin's mechanism of action. As a proof of principle we describe such an extension based on the kinetics of cisplatin incorporation into CAL 27 cells, another head and neck cancer cell line for which there is intracellular data.

4.1. **Extension of the intracellular cisplatin model.** In [37] data is presented that describes the intracellular cisplatin concentrations after both influx and efflux experiments. For the influx experiments, cells were incubated at constant extracellular cisplatin concentrations. Cells were then collected at specific times after the start of cisplatin exposure in order to measure intracellular Pt accumulation. For the efflux experiments, cells were incubated for at a constant extracellular cisplatin concentration. At the end of the incubation period, the intracellular cisplatin concentration was measured. Given more complete intracellular data of this kind, we can extend our previously described intracellular cisplatin model (see Figure 2) to include three intracellular compartments instead of two.
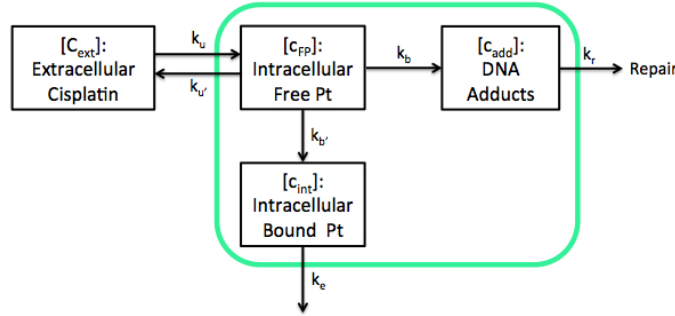
FIGURE 8. A possible extension to our intracellular cisplatin uptake model. This modification includes the addition of a third intracellular compartment that allows us to distinguish between cisplatin that is completely free (never been bound), cisplatin that is bound to non-DNA targets (the majority of intracellular cisplatin), and cisplatin that has formed DNA-adducts.

The new model allows us to distinguish between cisplatin that is completely free (never having been bound to an intracellular species), DNA-bound cisplatin, and cisplatin bound to non-DNA targets, which makes up approximately $75 - 95\%$ of all intracellular platinum [35]. A best fit of this modified model to the 2.5 μg/ml cisplatin dose data in [37] is shown in Figure 9. These simulations highlight the need for additional intracellular data for the specific experimentally cell lines under investigation in order to get a more complete picture of the drug-induced cell death kinetics. They also showcase the flexibility of the framework to be adapted once this data is regularly available.
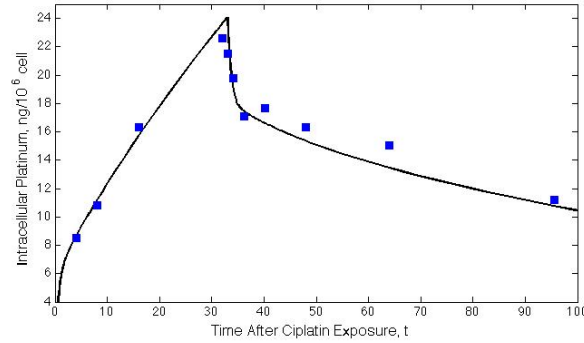

FIGURE 9. Best fit of the modified intracellular cisplatin model given in Figure 9 to the experimental data in [37] as shown in Figure 8.

4.2. **Extensions of the cellular model for cisplatin therapy.** The mechanisms linking the well described formation of cisplatin-DNA-adducts to the downstream events of programmed cell death are not yet well defined. Cell cycle arrest and the G2/M checkpoint have been suggested to be involved in apoptosis induction

in a variety of proliferating cells treated with cisplatin [10, 24, 32]. Research also shows that cisplatin-DNA adducts activate cell cycle check-point machinery that can delay entry to S-phase (halt at the G1 checkpoint), slow the replication of damaged DNA (intra-S checkpoint), and prevent entry to mitosis while damage persists (G2 checkpoint). When DNA synthesis is inhibited, the onset of mitosis can be delayed until DNA replication is complete (S/M checkpoint) [33]. These findings suggest possible amendments to the cellular model for cisplatin therapy that include the specifics of cell cycle interruption. An example of such a model is given schematica
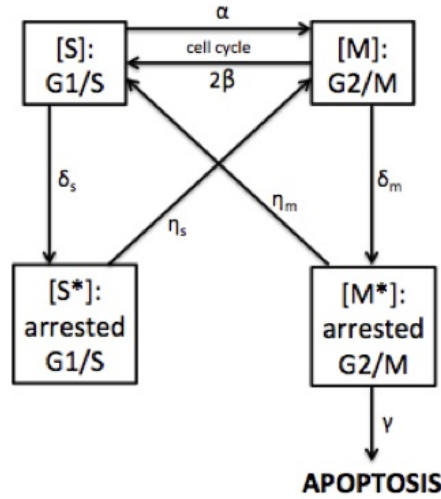

FIGURE 10. A possible extension to our cellular cisplatin uptake model. This modification includes the addition of progression through the cell cycle.

A model like the one in Figure 10 assumes that all cancers cells are proliferating cells - i.e. none of these cells are in the G0 phase of the cell cycle. These cancer cells are therefore divided into cells that are in the G1/S phase and cells that are in G2/M. Cells in G2/M have successfully copied their DNA, whereas cells in G1/S have not. Cisplatin acts to damage the DNA in all phases of the cell cycle, leading to cell cycle arrest. Following arrest, cells either are repaired and progress in the cell cycle or die. Experimental evidence suggests that cells recover and re-enter the cell cycle when treated with low concentrations of cisplatin, and cells treated with higher doses (or cells that are less resistant to cisplatin) remain arrested until death [32]. As detailed intracellular data becomes available, the potential exists to extend our work to developing a model that captures these dynamics.

4.3. **Extensions of the model for BM-1197 therapy.** It is widely reported that the outcome of death signals that are regulated by the Bcl-2 family depends upon a complex three-way ratio of the multi-domain anti-apoptotic, multi-domain pro-apoptotic, and BH3-only members. Specifically, Bax and Bak (multi-domain pro-apoptotic members) represent the central core of the proapoptotic Bcl-2 death machinery that is held in check by the pro-survival members Bcl-2 and Bcl-xL.

However, members of the BH3-only subfamily are required for the activation of proapoptotic Bax/Bak function [4]. Further, there is evidence that BH3-only members function upstream of Bax and Bak [20, 39] and that the killing effect of BH3-only members depends on Bax/Bak [34]. The model of BM-1197 therapy presented here could easily be extended to include additional members of the Bcl-2 family of proteins in order to quantify the influence of their interactions on tumor cell death.

4.4. **Extensions to in vivo therapy.** We have already developed a mathematical framework that describes tumor angiogenesis, vascular tumor growth, and response to therapies that target pro-apoptotic member of the Bcl-2 family [13, 14]. This model operates at the following levels: (1) Intracellular level: regulation of signaling pathways that are critical to endothelial cell proliferation, apoptosis, and migration; (2) Cellular level: cell-surface dynamics of receptor-ligand binding and receptor activation that lead to intracellular signal transduction cascades; and (3) Tissue level: dynamics of signaling chemicals and anti-cancer agents within the tissue, tumor growth dynamics, and tumor and vascular response to treatment. Results from this model underscore the potential of this model as a predictive tool to guide experiments aimed at testing novel anti-cancer therapies in vivo. The potential exists to integrate the *in vitro* model presented in this paper into our larger *in vivo* framework described above [13, 14]. This would allow us to quantify the potential of BM-1197 to retard tumor growth and reduce tumor vascularization *in vivo*. Further we could re-optimize the combination therapy for the *in vivo* setting and determine whether the optimized schedule for combination therapy predicted *in vitro*produces the desired synergy *in vivo*.

5. **Conclusion.** We have developed a mathematical model to explore the synergism between the widely used traditional chemotherapeutic agent, cisplatin, and the newly developed, dual action small molecule inhibitor of Bcl-2 and Bcl-xL, BM-1197. The model integrates the intracellular mechanism of action of both drugs, with a model of the tumor's response to treatment. To our knowledge this is the first model of cancer treatment that considers the intracellular mechanism of action of combined traditional and targeted therapies. Our model for BM-1197 is similar those presented in [13, 14, 12]. In particular, [12] developed a model for ovarian cancer treated with a combination of carboplatin and ABT-737, a small-molecule inhibitor of Bcl-2/Bcl-xL. In this model, a fully external treatment of cisplatin and its effect on cell death is used, in contrast to the intracellular mechanism of action model presented here. Based on simulations of our model, if we use only the external levels of cisplatin to determine cell death, this leads to very different values of the cell kill parameters and an underestimation of the IC50. Our model predicts that cisplatin sensitizes cancer cells for treatment with BM-1197 and these results are consistent with those presented in [12], where combination treatment was considered but the intracellular mechanism of action of the chemotherapeutic agent was not. One limitation associated with the approach presented here is that the experimental data on cytotoxicity used to build the model are all dose-response curves for a single exposure time. In the absence of additional data of this type, or even more ideal, time course data, parameters had to be estimated using two different data sets. This could potentially impact our conclusions concerning schedule dependence. However, given that our results are very consistent with existing models in the literature, we do not except qualitative differences in the predictions presented here had more data on UMSCC-74B cells been available. A highlight of

the framework presented here is that it is simple, yet extremely flexible. The extensions described above highlight its potential to be further developed as a predictive tool to guide experiments aimed at testing novel anti-cancer therapies, alone and in combination, at the intracellular and cellular levels both *in vitro* and *in vivo*.

REFERENCES

[1] J. M. Adams and S. Cory, The Bcl-2 protein family: Arbiters of cell survival, *Science*, **281** (1998), 1322–1326.

[2] L. Bai, J. Chen, D. McEachern, L. Liu and H. Zhou et al., BM-1197: A novel and specific bcl-2/bcl-xl inhibitor inducing complete and long-lasting tumor regression in vivo, *PLoS One*, **9** (2014), e99404.

[3] A. Basu and S. Krishnamurthy, BH3-only Bcl-2 family member Bim is required for apoptosis of autoreactive thymocytes, *Nature*, **415** (2002), 922–926.

[4] P. bouillet, J. F. Purton, D. I. Godfrey et al., BH3-only proteins and their roles in programmed cell death, *Oncogene*, **27** (2009), S128–S136.

[5] D. T. Chao and S. J. Korsmeyer, Bcl-2 family: Regulators of cell death, *Annu. Rev. Immunol.*, **16** (1998), 395–419.

[6] G. Chu, Cellular responses to cisplatin: The roles of dna-binding proteins an DNA repair, *J. Biol. Chem.*, **269** (1994), 787–790.

[7] A. W. El-Kareh and T. W. Secomb, A mathematical model for cisplatin cellular pharmacodynamics, *Neoplasia*, **5** (2003), 161–169.

[8] A. Florea and D. Busselberg, Cisplatin As An Anti-Tumor Drug: Cellular mechanisms of activity, drug resistance and induced side effects, *Cancers*, **3** (2011), 1351–1371.

[9] K. V. Floros, H. Thomadaki, G. Lallas, N. Katsaros, M. Talieri and A. Scorilas, Cisplatin-induced apoptosis in HL-60 human promyelocytic leukemia cells: differential expression of BCL2 and novel apoptosis-related gene BCL2L12, *Ann NY Acad Sci*, **1010** (2003), 153–158.

[10] V. M. Gonzalez, M. A. Fuertes, C. Alonso and J. M. Perez, Is Cisplatin-Induced Cell Death Always Produced by Apoptosis?, *Mol. Pharmacol.*, **59** (2001), 657–663.

[11] H. V. Jain, A. Richardson, M. Meyer-Hermann and H. M. Byrne, Exploiting the synergy between carboplatin and ABT-737 in the treatment of ovarian carcinomas, *PLoS One*, **9** (2014), e81582.

[12] H. V. Jain and M. Meyer-Hermann, The molecular basis of synergism between carboplatin and ABT-737 therapy targeting ovarian carcinomas, *Cancer Res.*, **71** (2011), 705–715.

[13] H. V. Jain, J. E. Nor and T. L. Jackson, Quantification of endothelial cell-targeted anti-Bcl-2 therapy and its suppression of tumor growth and vascularization, *Mol. Cancer There.*, **8** (2009), 2926–2936.

[14] H. V. Jain, J. E. Nor and T. L. Jackson, Modeling the VEGF-Bcl-2-CXCL8 pathway in intratumoral agiogenesis, *Bull. Math. Biol.*, **70** (2008), 89–117.

[15] Z. Jiang, X. Zheng and K. M. Rich, Down-regulation of Bcl-2 and Bcl-xL expression with bispecific antisense treatment in glioblastoma cell lines induce cell death, *J Neurochem*, **84** (2003), 273–281.

[16] Y. Jung and S. J. Lippard, Direct Cellular Responses to Platinum-Induced DNA Damage, *Chem. Rev.*, **107** (2007), 1387–1407.

[17] A. Kothandapani, V. S. Dangeti and A. R. Brown, et al., Novel role of base excision repair (BER) in mediating cisplatin cytotoxicity, *J. Biol. Chem.*, **286** (2011), 14564–14574.

[18] Q. T. Le and A. J. Giaccia, Therapeutic exploitation of the physiological and molecular genetic alterations in head and neck cancer, *Clin. Cancer Res.*, **9** (2003), 4287–4295.

[19] J. Y. Li, Y. Y. Li, W. Jin, Q. Yang, Z. M. Shao and X. S. Tian, ABT-737 reverses the acquired radioresistance of breast cancer cells by targeting Bcl-2 and Bcl-xL, *J. Exp Clin. Cancer Res.*, **31** (2012), p102.

[20] T. Lindsten, A. J. Ross and A. King et al., The combined functions of proapoptotic Bcl-2 family members bak and bax are essential for normal development of multiple tissues, *Mol. Cell.*, **6** (2000), 1389–1399.

[21] S. R. McWhinney, R. M. Goldberg and H. L. McLeod, Platinum neurotoxicity pharmacogenetics, *Mol. Cancer Ther.*, **8** (2009), 10–16.

[22] D. Mitra, S. P. Malkoski and X. Wang, Cancer stem cells in head and neck cancer, *Cancers*, **3** (2011), 415–427.

[23] M. J. Mokhtari, A. Akbarzadeh and M. Hashemi et al., Cisplatin induces down regulation of BCL2 in T47D breast cancer cell line, *Adv Studies in Biol*, **4** (2012), 19–25.

[24] S. Mueller, M. Schittenhelm and F. Honecker, et al., Cell-cycle progression and response of germ cell tumors to cisplatin in vitro, *Int. J. Oncol.*, **29** (2006), 471–479.

[25] D. W. Nicholson, From bench to clinic with apoptosis-based therapeutic agents, *Nature*, **407** (2000), 810–816.

[26] D. Park, A. T. Magis and R. Li et al., Novel small-molecule inhibitors of Bcl-XL to treat lung cancer, *Cancer Res.*, **73** (2013), 5485–5496.

[27] D. Pulte and H. Brennera, Changes in survival in head and neck cancers in the late 20th and early 21st century: A period analysis, *Oncologist*, **15** (2010), 994–1001.

[28] J. C. Reed, Apoptosis-based therapies, *Nat. Rev. Drug Discov.*, **1** (2002), 111–121.

[29] J. C. Reed, Bcl-2 family proteins: Strategies for overcoming chemoresistance in cancer, *Adv. in Pharm.*, **41** (1997), 501–532.

[30] A. W. Roberts, J. F. Seymour and J. R. Brown et al., Substantial susceptibility of chronic lymphocytic leukemia to BCL2 inhibition: Results of a phase I study of navitoclax in patients with relapsed or refractory disease, *J. Clin. Oncol.*, **30** (2012), 488–496.

[31] S. Y. Sharp, P. M. Rogers and L. R. Kelland, Transport of cisplatin and bis-acetato-amminedichlorocyclohexylamine Platinum(IV) (JM216) in human ovarian carcinoma cell lines: identification of a plasma membrane protein associated with cisplatin resistance, *Clin. Cancer Res.*, **1** (1995), 981–989.

[32] C. M. Sorenson, M. A. Barry and A. Eastman, Analysis of events associated with cell cycle arrest at G2 phase and cell death induced by cisplatin, *JNCI.*, **82** (1990), 749–755.

[33] J. Smith, L. M. Tho, N. Xu and D. A. Gillespie, The ATM-Chk2 and ATR-Chk1 pathways in DNA damage signaling and cancer, *Adv. Cancer Res.*, **108** (2010), 73–112.

[34] G. C. Shore and J. Viallet, Modeling the bcl-2 family of apoptosis suppressors for potential herapeutic benefit in cancer, *Hemotol.*, **1** (2005), 226–230.

[35] V. Sresht, J. R. Bellare and S. K. Gupta, Modeling the cytotoxicity of cisplatin, *Ind. Eng. Chem. Res.*, **50** (2011), 12872–12880.

[36] K. A. Tacka, D. Szalda, A. K. Souid, J. Goodisman and J. C. Dabrowiak, Experimental and theoretical studies on the pharmacodynamics of cisplatin in jurkat cells. *Chem. Res. Toxicol.*, **17** (2004), 1434–1444.

[37] V. Troger, J. L. Fischel and P. Formento et al., Effects of prolonged exposure to cisplatin on cytotoxicity and intracellular drug concentration, *Eur. J. Cancer*, **28** (1992), 82–86.

[38] C. Tse, A. R. Shoemaker and J. Adickes et al., ABT-263: A potent and orally bioavailable Bcl-2 family inhibitor, *Cancer Res.*, **68** (2008), 3421–3428.

[39] M. C. Wei, W. X. Zong and E. H. Cheng et al., Proapoptotic BAX and BAK: A requisite gateway to mitochondrial dysfunction and death, *Scient*, **292** (2001), 727–730.

E-mail address: alexis_cook@brown.edu

E-mail address: ziazadeh@umich.edu

E-mail address: jialu@med.umich.edu

E-mail address: tjacks@umich.edu